## Electronic, structural and magnetic properties of Mn(1+x)Pt(1-x)Sb

Abdullah Al Maruf,<sup>1</sup> Adam Ramker,<sup>2</sup> Shah Valloppilly,<sup>3</sup> Paul M. Shand,<sup>2</sup> Pavel V. Lukashev,<sup>2#</sup> and Parashu Kharel<sup>1\*</sup>

<sup>1</sup>Department of Physics, South Dakota State University, Brookings, SD 57007

<sup>2</sup>Department of Physics, University of Northern Iowa, Cedar Falls, Iowa 50614

<sup>3</sup>Nebraska Center for Materials and Nanoscience, University of Nebraska, Lincoln, NE 68588

#pavel.lukashev@uni.edu

\*parashu.kharel@sdstate.edu

#### **Abstract**

Electronic and magnetic properties of half-metallic Heusler alloys can be modified by tuning their chemical compositions. We have carried out a combined theoretical and experimental investigation of  $Mn_{(1+x)}Pt_{(1-x)}Sb$  ( $0 \le x \le 0.5$ ) alloys. Our first-principles calculations indicate that the stoichiometric MnPtSb exhibits nearly half-metallic band structure, but a robust half-metallicity can be achieved in Mn-rich compositions  $Mn_{(1+x)}Pt_{(1-x)}Sb$  ( $0 \le x \le 0.5$ ) with x = 0.25 and higher in their cubic structures. In addition, while MnPtSb exhibits ferromagnetic alignment,  $Mn_{(1+x)}Pt_{(1-x)}Sb$  is ferrimagnetic for all non-zero values of x. We have also synthesized cubic MnPtSb and  $Mn_{1.25}Pt_{0.75}Sb$  alloys using arc melting and annealing. The magnetic properties of these alloys are consistent with our theoretical predictions. These results indicate that the Mn-rich  $Mn_{(1+x)}Pt_{(1-x)}Sb$  alloys have potential for spin-transport-based devices.

#### I. Introduction

Half-metallic (HM) Heusler alloys have been studied extensively for applications in spin-transport-based devices because of their high Curie temperature, as these materials could exhibit a complete spin polarization at room temperature. 1,2,3,4,5,6,7,8,9,10,11,12,13 More specifically, a significant amount of recent research is focused on tuning the spin polarization and other magnetic properties of these alloys with external stimuli, such as chemical substitution, 14 mechanical strain, 15 surface termination, 16 atomic disorder, 17,18,19,20 temperature, 21 stoichiometry, 22 etc. The

purpose of the current work is to study how the electronic, structural and magnetic properties of MnPtSb change as the Mn and Pt compositions are varied.

MnPtSb belongs to a family of half-Heusler alloys. In addition to other various magnetic applications, Heusler alloys have been extensively studied for spin-transport-based device applications, because some of them exhibit half-metallic band structure and small magnetization due to compensated ferrimagnetic arrangements with high Curie temperature much higher than room temperature. <sup>23,24,25,26,27,28</sup> The main advantage of compensated ferrimagnetism is that the materials exhibiting this arrangement produce no stray magnetic fields due to their small or zero net magnetizations. These materials are more favorable for nanoelectronic devices because they cause no interference in the neighboring magnetic elements. However, half-metallic Heusler alloys exhibiting ferromagnetic ordering with moderate magnetizations have also been used as electrodes in tunnel junctions to generate spin polarized electrons.<sup>29</sup> Some of these alloys, for example IrMnSb and MnPtSb have been reported to exhibit nearly half-metallic electronic structure, where the Fermi level crosses the minority-spin valence states at the edge of energy gap. 30,1,11 For such materials, it may be possible to induce a half-metallic transition by some external stimuli, such as mechanical strain, chemical substitution, etc. This approach is relatively well studied, albeit, mostly theoretically.<sup>30</sup> It is not very difficult to achieve half-metallic transition by simply manipulating the lattice parameter (either directly, or by chemical substitution), especially if the band crossing at the Fermi level is relatively small. Here, we explore a slightly different situation, namely the effect of stoichiometry on the electronic and magnetic properties of  $Mn_{(1+x)}Pt_{(1-x)}Sb$ alloys. We show that while the parent alloy MnPtSb is nearly half-metallic, a robust halfmetallicity can be achieved in  $Mn_{(1+x)}Pt_{(1-x)}Sb$  with x = 0.25 and higher.

The rest of the paper is organized as follows. Section II outlines the computational and experimental methods. Both the theoretical and experimental results are discussed in section III. Section IV contains concluding remarks, and is followed by acknowledgments and references.

# II. Experimental and Computational Methods

#### a. Computational Methods

We used the projector augmented-wave method (PAW)<sup>31</sup> within the Perdew-Burke-Ernzerhof (PBE) generalized-gradient approximation (GGA)<sup>32</sup>, implemented in the Vienna *ab*  initio simulation package (VASP).<sup>33</sup> The cut-off energy of the plane-waves is set to 500 eV, and the integration method<sup>34</sup> with a 0.05 eV width of smearing is used. The structural optimization was performed with the energy convergence criteria of 10<sup>-2</sup> meV. The total energy and electronic structure calculations were performed with a stricter convergence criteria of 10<sup>-3</sup> meV. The Brillouin-zone integration was performed with a k-point mesh of 12 × 12 × 12. Some of the results and figures were obtained using the MedeA® software environment.<sup>35</sup> More advanced computational techniques, such as hybrid functionals or GW method are not used in this work, since the minority-spin band gap of half-metallic Heusler compounds is usually adequately estimated with regular PBE functionals. For example, Meinert et al. showed in that GW and PBE result in essentially the same minority-spin energy gap of Co<sub>2</sub>MnSi, which is one of the first experimentally confirmed half-metallic compound.<sup>36</sup>

The calculations were performed using Extreme Science and Engineering Discovery Environment (XSEDE) resources located at the Pittsburgh Supercomputing Center (PSC)<sup>37</sup>, and the resources of the Center for Functional Nanomaterials (CFN) at Brookhaven National Laboratory (BNL).

## b. Experimental Methods

MnPtSb and Mn<sub>1.25</sub>Pt<sub>0.75</sub>Sb ingots were prepared using arc-melting and high-vacuum annealing. First, pieces of highly pure (99.99%) Mn, Pt, and Sb with proper weight ratio were cut from corresponding commercially available pellets and melted on a water-cooled Cu hearth of an arc furnace in an argon environment. An additional 2% of Mn by weight was used to compensate the weight loss during the arc-melting.<sup>38</sup> The subsequent annealing of each sample was performed in a tubular vacuum furnace ( $\sim 10^{-7}$  torr) at 700°C for 24 hours to further homogenize the samples. The crystal structures of the samples were analyzed using Rigaku MiniFlex600 x-ray diffractometer with Cu-K $\alpha$  source ( $\lambda = 1.54$  Å). The elemental compositions of the annealed samples were confirmed using Energy-dispersive x-ray spectroscopy (EDS). The exact elemental compositions as determined by EDS are MnPt<sub>1.04</sub>Sb<sub>0.96</sub> and Mn<sub>1.27</sub>Pt<sub>0.71</sub>Sb<sub>1.02</sub> which are very close to the nominal compositions. A Quantum Design VersaLab magnetometer was used to investigate the magnetic properties.

### III. Results

## a. Computational Results

Half-Heusler alloys, such as MnPtSb, can crystallize in two phases:  $\alpha$ -phase, and  $\gamma$ -phase (see Figure 1). These two phases may exhibit distinctly different electronic and magnetic properties, see e.g. Shaughnessy, *et al.*, and references therein.<sup>39</sup> In experiment, MnPtSb has been synthesized in the  $\alpha$ -phase, which is consistent with our calculations.<sup>40</sup> In particular, the calculated energies per 12-atom cell are -81.295177 eV for  $\alpha$ -phase and -78.074059 eV for  $\gamma$ -phase. The calculated lattice parameters are a = 6.228 Å and a = 6.121 Å for the  $\alpha$ - and  $\gamma$ -phases, respectively. Our calculations also indicate that there is no transition from  $\alpha$ -phase to  $\gamma$ -phase in a realistically attainable range of external pressure. Therefore, in the rest of this work, we focus on the  $\alpha$ -phase of this material.

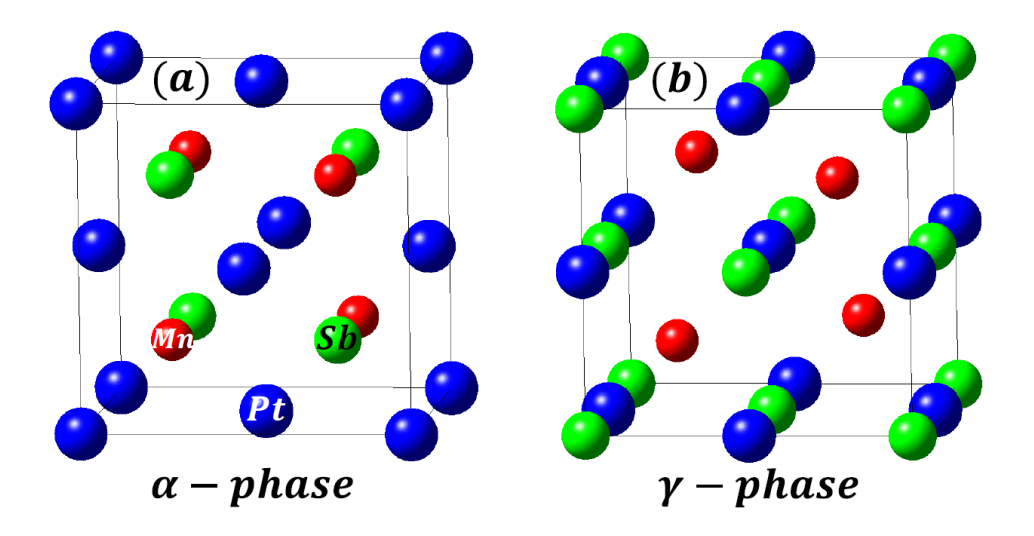


Figure 1: Crystal structures of  $\alpha$ -phase (a), and  $\gamma$ -phase (b) of MnPtSb. Atoms are color-coded as indicated in the figure (blue – Pt, red – Mn, green – Sb).

Figure 2 shows the calculated total and element-resolved density of states (DOS) of MnPtSb. It is clear from the DOS of Fig. 2 that the stoichiometric MnPtSb is not completely half-metallic as the Fermi level crosses the minority-spin valence states. The main contribution to the minority-spin states at the Fermi energy comes from Mn (see inset of Fig. 2), with Pt and Sb having significantly smaller contributions. Nearly half-metallic electronic structure have been previously reported for other Heusler alloys with similar lattice symmetry. For example, in our recent work, we have shown that a robust half-metallic transition can be achieved in a nearly half-metallic CrMnSb by a partial substitution of Sb with P, which essentially mimics an external uniform

mechanical pressure.<sup>30</sup> Alternatively, the electronic band structure of a nearly half-metallic alloy such as MnPtSb can be modified by tuning its stoichiometry leading to a robust half-metallic state. The main difference here is that by varying Mn / Pt ratio in MnPtSb, one naturally tunes the magnetization of this material, while the atomic substitution of non-magnetic atom (Sb) has no direct effect on the magnetic structure. Indirectly, it may still change the magnetic structure due to the change in volume of the unit cell.

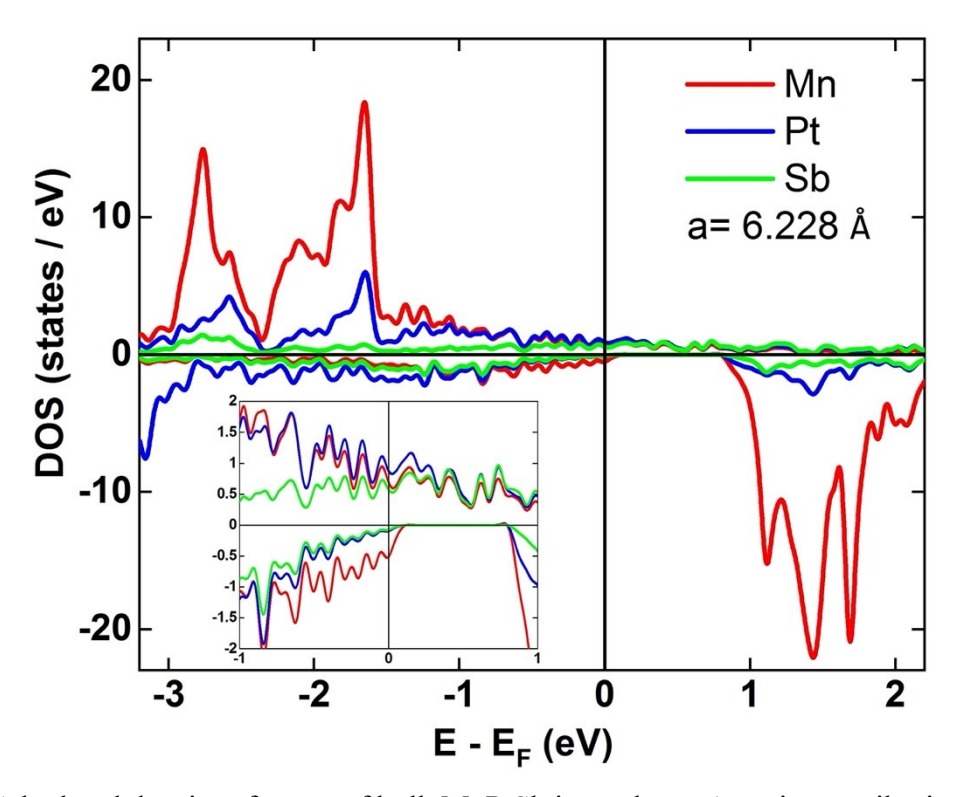


Figure 2: Calculated density of states of bulk MnPtSb in  $\alpha$ -phase. Atomic contributions are color-coded as indicated in the figure. The inset shows an enlarged version of the figure, around the Fermi level. Positive and negative DOS correspond to majority- and minority- spin states, respectively.

Figure 3 summarizes the calculated DOS (a), lattice parameter (b), and spin-polarization and magnetization (c) of  $Mn_{(1+x)}Pt_{(1-x)}Sb$  ( $0 \le x \le 0.5$ ). As shown in Fig. 3(a), a robust half-metallic transition takes place when 25 percent of Pt sites are replaced with Mn atoms. In addition,  $Mn_{(1+x)}Pt_{(1-x)}Sb$  remains completely half-metallic when 50 percent of Pt sites are replaced with Mn atoms. Since the atomic radius of Mn is smaller than that of Pt, there is a systematic decrease in the lattice parameters of  $Mn_{(1+x)}Pt_{(1-x)}Sb$  as the value of x increases (Fig. 3 (b)). However,  $Mn_{(1+x)}Pt_{(1-x)}Sb$  maintains cubic or nearly cubic symmetry for all calculated values of x. This has

been tested by explicitly imposing a biaxial strain on each of these cells. The cubic structure turns out to be a lower energy state for all considered cases, except for x = 0.5, where a small tetragonal distortion could be feasible. In particular, for x = 0.5, the optimized lattice parameters are a = b = 6.091 Å; c = 6.156 Å. The lattice constants marked in figures 3 (a) and (b) correspond to the average of these two values. This suggests that a physical mechanism governing the half-metallic transition is the reduction of unit cell volume, consistent with earlier reports on similar materials.  $^{11,30}$ 

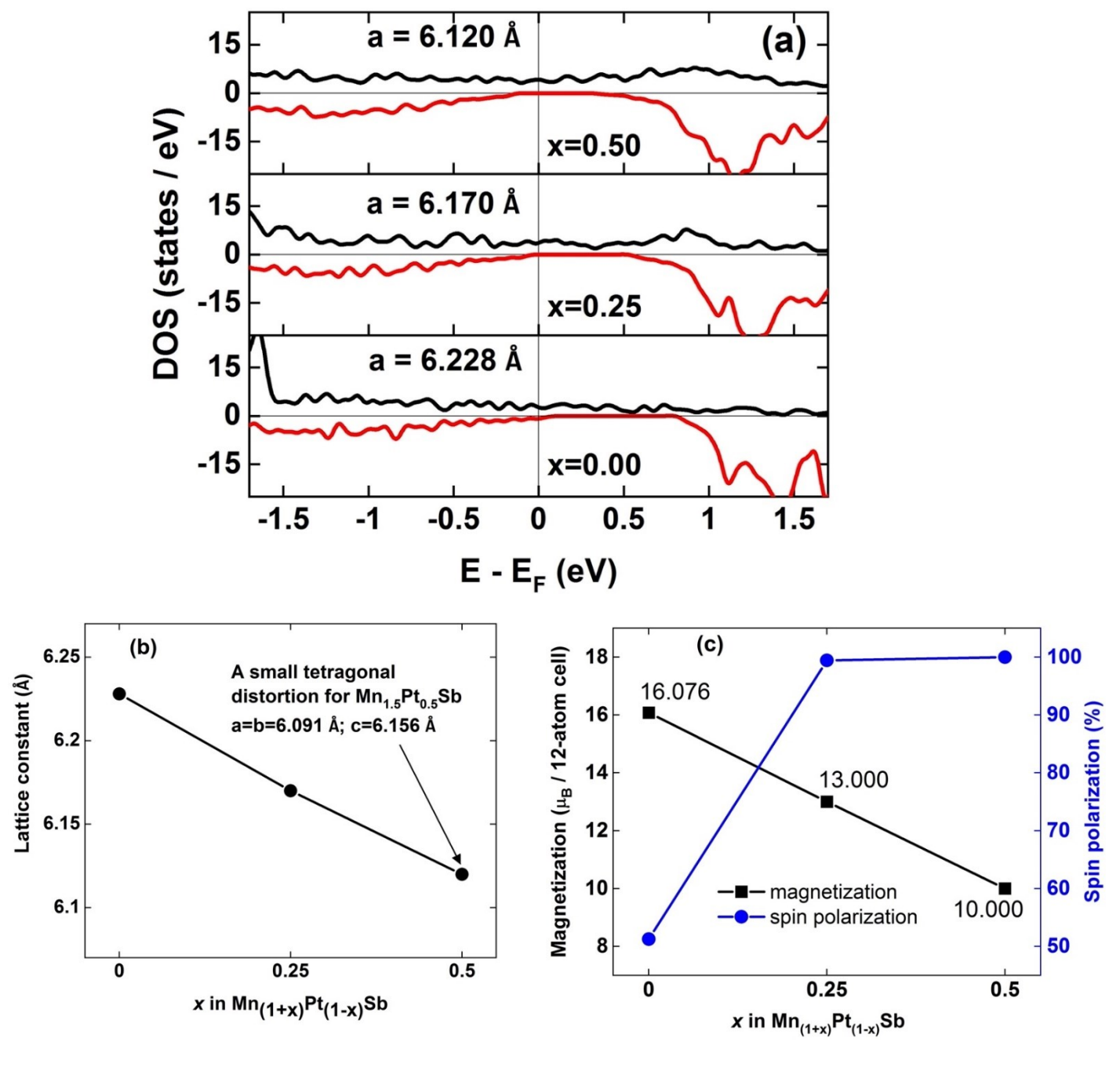


Figure 3: (a) Calculated density of states of bulk  $Mn_{(1+x)}Pt_{(1-x)}Sb$ . Particular values of x, as well as corresponding optimized lattice parameters are shown in the figure. Positive and negative DOS correspond to majority- and minority- spin states, respectively. (b) Calculated lattice constants of bulk  $Mn_{(1+x)}Pt_{(1-x)}Sb$ . (c) Calculated spin-polarization (blue line and circles) and magnetization in terms of magnetic moment per 12-atom cell (black line and squares with numerical values shown) of bulk  $Mn_{(1+x)}Pt_{(1-x)}Sb$  ( $0 \le x \le 0.5$ ).

Fig. 3 (c) shows calculated spin-polarization and magnetization (magnetic moment per 12-atom cell) of  $Mn_{(1+x)}Pt_{(1-x)}Sb$ , for different values of x. Here, the spin polarization is calculated as  $P = (N_{\uparrow}(E_F) - N_{\downarrow}(E_F))/(N_{\uparrow}(E_F) + N_{\downarrow}(E_F))$ , where  $N_{\uparrow}(E_F)$  and  $N_{\downarrow}(E_F)$  are the spin-dependent density of states (DOS) at the Fermi level,  $E_F$ . The degree of spin polarization reaches 100% when x reaches x = 0.25 and remains 100% for x = 0.5 as well. In addition, the calculated magnetization values of  $Mn_{(1+x)}Pt_{(1-x)}Sb$  for  $0.25 \le x \le 0.5$  are integral, supporting the half-metallic states in these compounds. The integral magnetization is a result of the Fermi energy falling on the band gap of one of the spin channels making all the states in the corresponding valence band occupied. Since the total number of these occupied states is an integer, the resulting magnetic moment is also an integer. Further, the magnetization of  $Mn_{(1+x)}Pt_{(1-x)}Sb$  shows a systematic decrease with the increase in the value of x. This happens as the Mn moments in the Pt site antialign with the Mn moments in the regular Mn sites. In particular, while MnPtSb is ferromagnetic with magnetic moment of about  $3.9 \mu_B/Mn$ ,  $Mn_{(1+x)}Pt_{(1-x)}Sb$  is ferrimagnetic for all non-zero values of x. We also note that the Mn moments at regular Mn sites and Pt sites have different absolute values with  $3.6 \mu_B/Mn$  and  $2.6 \mu_B/Mn$  at Mn and Pt sites, respectively.

# b. Experimental Results

We have investigated the crystal structure and magnetic properties of MnPtSb and Mn<sub>1.25</sub>Pt<sub>0.75</sub>Sb alloys. We also prepared samples with higher concentration of *x* but they all show large amount of Mn<sub>2</sub>Sb impurity phase. Therefore, here we have reported the data recorded only on MnPtSb and Mn<sub>1.25</sub>Pt<sub>0.75</sub>Sb.

Figure 4 shows the room temperature x-ray diffraction patterns of MnPtSb and  $Mn_{1.25}Pt_{0.75}Sb$  alloys. As shown in Fig. 4(a), the XRD pattern contains diffraction peaks from purely cubic structure (F $\overline{4}$ 3m), which agrees well with the theoretical prediction. The main peaks in the XRD pattern of  $Mn_{1.25}Pt_{0.75}Sb$  are also indexed with cubic Heusler structure. However, the

XRD profile analysis indicates that there is a small amount (less than 5 % by weight) of Mn<sub>2</sub>Sb impurity phase. The peaks corresponding to Mn<sub>2</sub>Sb are marked with star sign in the pattern. The

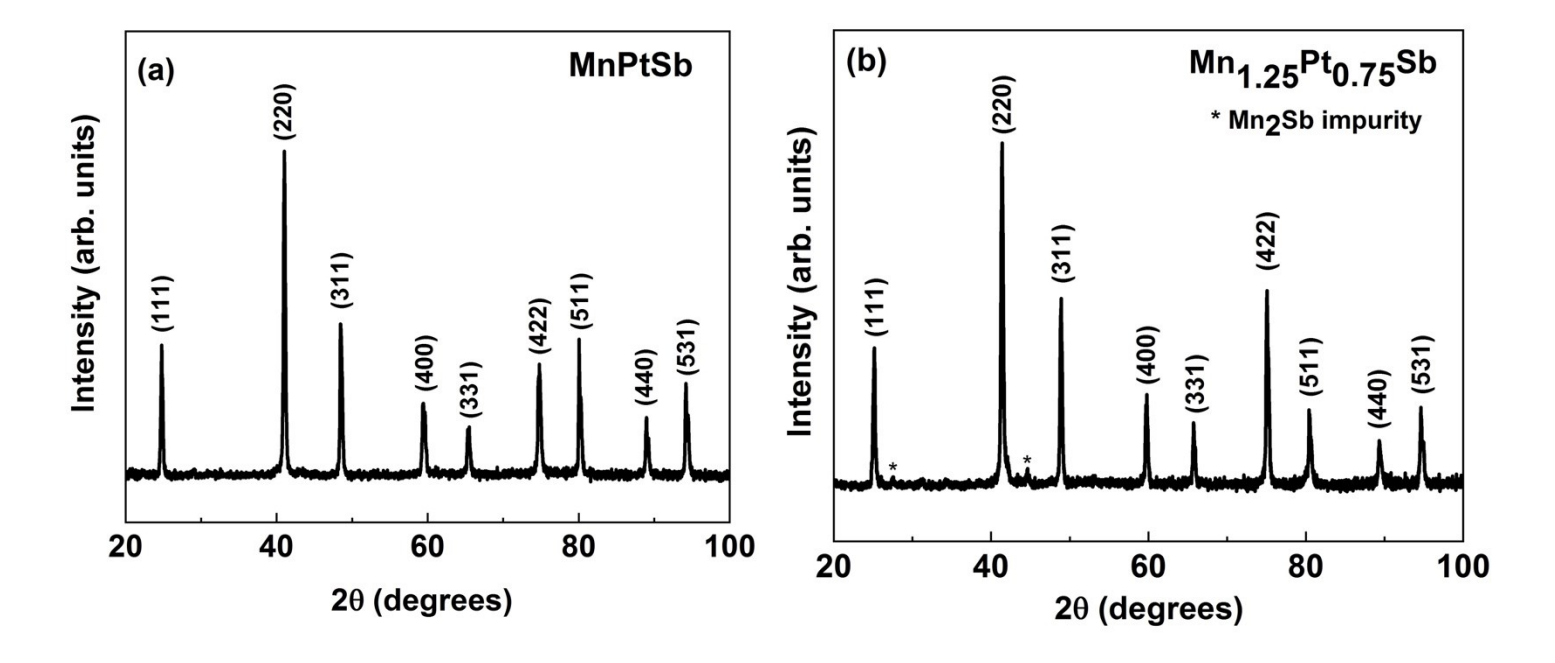


Figure 4: Room temperature powder x-ray diffraction patterns of (a) MnPtSb and (b)  $Mn_{1.25}Pt_{0.75}Sb$  alloys. In figure (b), the peaks marked with star sign are from  $Mn_2Sb$  impurity phase.

lattice parameters of MnPtSb and Mn<sub>1.25</sub>Pt<sub>0.75</sub>Sb obtained from the profile analysis of XRD patterns are 6.221 Å and 6.218 Å, respectively. The experimental lattice parameter of MnPtSb agrees well with the theoretical value (6.228 Å) but that of Mn<sub>1.25</sub>Pt<sub>0.75</sub>Sb is slightly larger than the equilibrium lattice constant predicted by our first principles calculations (6.170 Å). Our first principles calculations also indicate that the substitution of some of Sb sites by Mn due to disorder may increase lattice parameters of these alloys (details of the calculation are not shown here). We attribute this discrepancy in lattice parameter of Mn<sub>1.25</sub>Pt<sub>0.75</sub>Sb to the atomic site disorder, which is common in Heusler alloys.

The temperature and magnetic field dependence of magnetization of MnPtSb and Mn<sub>1.25</sub>Pt<sub>0.75</sub>Sb alloys are shown in Figures 5 (a) and (b), respectively. Figure 5 (a) shows the thermomagnetic curves M(T) for the MnPtSb and Mn<sub>1.25</sub>Pt<sub>0.75</sub>Sb alloys recorded at 1 kOe. The M(T) curves of both the samples are similar to those of ferro- or ferrimagnetic materials. The Curie temperatures  $(T_C)$  determined from the lowest points in the corresponding dM/dT versus T curves,

as shown in the inset of Fig. 5(a), are 555 K and 530 K for MnPtSb and Mn<sub>1.25</sub> Pt<sub>0.75</sub>Sb, respectively. The  $T_C$  for MnPtSb is close to the value (582 K) reported in the literature.<sup>42</sup>

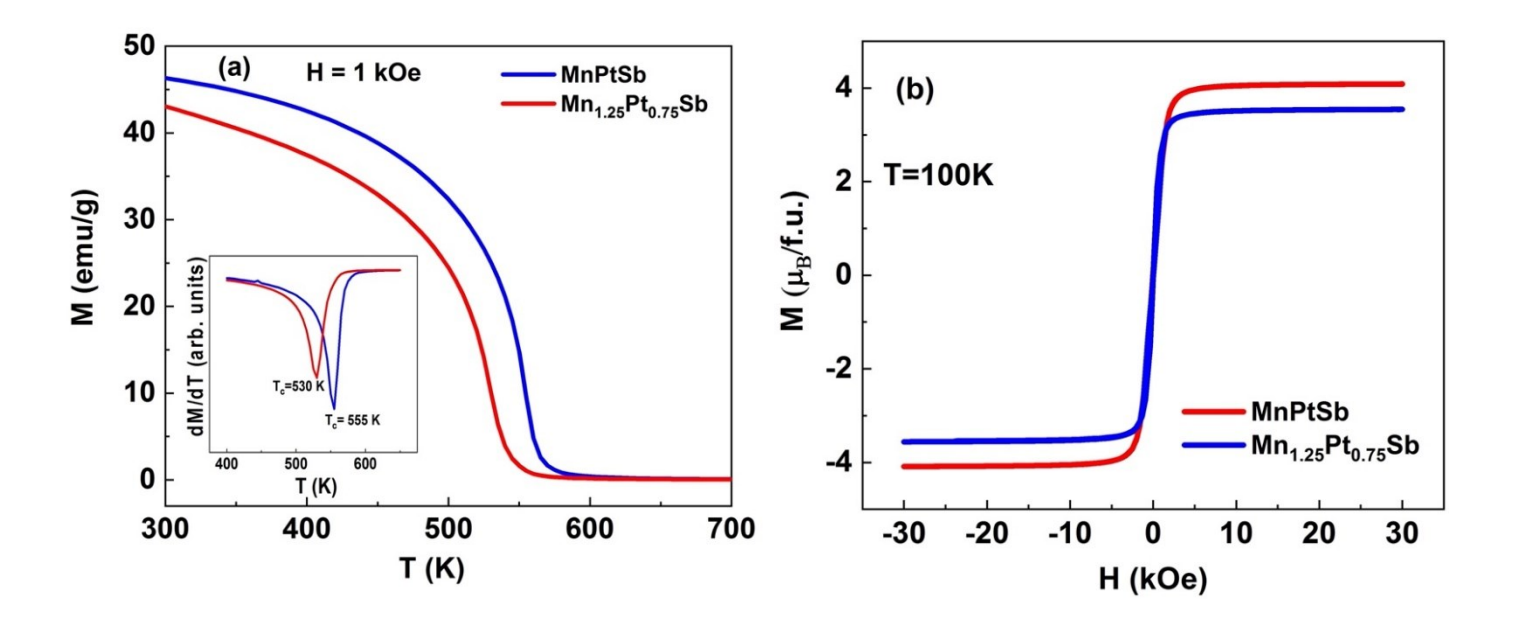


Figure 5: (a) The temperature dependence of magnetization M(T) of MnPtSb and Mn<sub>1.25</sub>Pt<sub>0.75</sub>Sb alloys measured at 1 kOe. Inset: dM/dT versus T plots. (b) The magnetic field dependence of magnetization M(H) of MnPtSb and Mn<sub>1.25</sub>Pt<sub>0.75</sub>Sb alloys measured at 100 K.

Although there is a small decrease in the Curie temperature due to a partial substitution of Mn in the Pt-site, it is still much higher than the room temperature. A small decrease in the Curie temperature could be attributed to the ferrimagnetic transition in Mn-rich samples, and possible atomic disorder. In particular, as discussed in the computational section, Mn-rich cells exhibit ferrimagnetic alignment with the smaller magnetic moment of Mn at the Pt sites and the antiferromagnetic exchange with the Mn ions at the regular sites. Thus, both the effective exchange strength and the average magnetic moment of Mn are reduced, which reduces  $T_C$ 

Figure 5(b) shows the isothermal magnetization M(H) curves for the MnPtSb and Mn<sub>1.25</sub>Pt<sub>0.75</sub>Sb alloys recorded at 100 K, which is close to the lowest attainable temperature in our VersaLab magnetometer. Both the compounds show soft magnetic behavior with very small coercivities of less than 25 Oe. The M(H) curves are completely saturated at 3 T magnetic field. The high-field magnetizations measured at 100 K are respectively 63 emu/g (4.08  $\mu$ B/f.u.) and 60 emu/g (3.54  $\mu$ B/f.u.) for MnPtSb and Mn<sub>1.25</sub>Pt<sub>0.75</sub>Sb, respectively. We used the experimental lattice

parameters and densities of the alloys to express their magnetizations in terms of  $\mu_B/f.u$ . The experimental value of high-field ( $\mu_0H=3$  T) magnetization of MnPtSb agrees well with the theoretical prediction (4.02  $\mu_B/f.u$ .), however, that of the Mn<sub>1.25</sub>Pt<sub>0.75</sub>Sb is slightly larger than the magnetic moment predicted by the first-principle calculations (3.25  $\mu_B/f.u$ .). We attribute this to the atomic site disorder as discussed in XRD analysis above. Our first principles calculations also indicate that the Mn moments in the Sb site align parallel and those in Pt site align antiparallel to the Mn moments in the regular Mn site. This competition may slightly increase total magnetization in Mn<sub>1.25</sub>Pt<sub>0.75</sub>Sb.

#### **IV.** Conclusions

We performed combined theoretical and experimental studies of electronic, structural and magnetic properties of  $Mn_{(1+x)}Pt_{(1-x)}Sb$  ( $0 \le x \le 0.5$ ) Heusler alloys. The density functional calculations predict that the compounds crystallize in cubic structure, and the compositions between x = 0.25 and x = 0.5 are fully half-metallic. Two of the theoretically studied compounds MnPtSb and  $Mn_{1.25}Pt_{0.75}Sb$  were synthesized, and their crystal structure and magnetic properties were investigated. Both the alloys show moderate saturation magnetizations, namely,  $4.08 \mu_B/f.u.$  for MnPtSb and  $3.54 \mu_B/f.u.$  for Mn<sub>1.25</sub>Pt<sub>0.75</sub>Sb with respective high Curie temperatures of 555 K and 530 K. The theoretical values of saturation magnetizations are  $4.02 \mu_B/f.u.$  for MnPtSb and  $3.25 \mu_B/f.u.$  for Mn<sub>1.25</sub>Pt<sub>0.75</sub>Sb. These results suggests that Mn<sub>1.25</sub>Pt<sub>0.75</sub>Sb may be useful for spintronics applications, where high spin-polarization, high Curie temperature, and moderate magnetization are desired.

### V. Acknowledgments

This research is supported by the *National Science Foundation* (NSF) under Grant Numbers 2003828 and 2003856 via DMR and EPSCoR. This work used the Extreme Science and Engineering Discovery Environment (XSEDE), which is supported by National Science Foundation grant number ACI-1548562. This work used the XSEDE Regular Memory (Bridges) and Storage (Bridges Pylon) at the Pittsburgh Supercomputing Center (PSC) through allocation TG-DMR180059, and the resources of the Center for Functional Nanomaterials, which is a U.S.

DOE Office of Science Facility, and the Scientific Data and Computing Center, a component of the Computational Science Initiative, at Brookhaven National Laboratory (BNL) under Contract No. DE-SC0012704.

#### References

\_

- <sup>3</sup> E. Şaşıoğlu, L. M. Sandratskii, P. Bruno, and I. Galanakis, Exchange interactions and temperature dependence of magnetization in half-metallic Heusler alloys, Phys. Rev. B **72**, (2005) 184415.
- <sup>4</sup> S. Picozzi, A. Continenza, and A. J. Freeman, Co<sub>2</sub>MnX (X=Si, Ge, Sn) Heusler compounds: An ab initio study of their structural, electronic, and magnetic properties at zero and elevated pressure, Phys. Rev. B **66**, (2002) 094421.
- <sup>5</sup> B. Balke, G. H. Fecher, J. Winterlik, and C. Felser, Mn<sub>3</sub>Ga, a compensated ferrimagnet with high Curie temperature and low magnetic moment for spin torque transfer applications, Appl. Phys. Lett. **90**, (2007) 152504.
- <sup>6</sup> H. Kurt, K. Rode, M. Venkatesan, P. Stamenov, and J. M. D. Coey, Mn3-xGa( $0 \le x \le 1$ ): Multifunctional thin film materials for spintronics and magnetic recording, Phys. Status Solidi B **248**, (2011) 2338.
- J. Winterlik, S. Chadov, A. Gupta, V. Alijani, T. Gasi, K. Filsinger, B. Balke, G. H. Fecher, C. A. Jenkins, F. Casper, J. Kübler, G. Liu, L. Gao, S. S. P. Parkin, C. Felser, Design Scheme of new tetragonal Heusler compounds for spin-transfer torque applications and its experimental realization, Adv. Mater. 24, (2012) 6283.
- <sup>8</sup> A. Nelson, P. Kharel, Y. Huh, R. Fuglsby, J. Guenther, W. Zhang, B. Staten, P. Lukashev, S. Valloppilly, and D. J. Sellmyer, Enhancement of Curie temperature in Mn<sub>2</sub>RuSn by Co substitution, J. Appl. Phys. 117, (2015) 153906.
- <sup>9</sup> I. Galanakis, Heusler Alloys (Springer Series in Materials Science, vol. 222) ed. C. Felser and A. Hirohata (Berlin: Springer, 2016).
- P. Lukashev, P. Kharel, S. Gilbert, B. Staten, N. Hurley, R. Fuglsby, Y. Huh, S. Valloppilly, W. Zhang, K. Yang, R. Skomski, and D. J. Sellmyer, Investigation of spin-gapless semiconductivity and half-metallicity in Ti<sub>2</sub>MnAl-based compounds, Appl. Phys. Lett. 108, (2016) 141901.
- <sup>11</sup> I. Tutic, J. Herran, B. Staten, P. Gray, T. R. Paudel, A. Sokolov, E. Y. Tsymbal, and P. V. Lukashev, Effects of pressure and strain on spin polarization of IrMnsb, J. Phys.: Condens. Matter **29**, (2017) 075801.
- <sup>12</sup> J. Herran, R. Carlile, P. Kharel, and P. Lukashev, Half-metallicity in CrAl-terminated Co<sub>2</sub>CrAl thin film, J. Phys.: Condens. Matter **31**, (2019) 495801.
- <sup>13</sup> R. Carlile, J. Herran, S. Poddar, E. Montgomery, P. Kharel, P. Shand, and P. Lukashev, Perpendicular magnetic anisotropy in half-metallic thin-film Co<sub>2</sub>CrAl, J. Phys.: Condens. Matter **33**, (2021) 105801.

<sup>&</sup>lt;sup>1</sup> R. A. de Groot, F. M. Mueller, P. G. van Engen, and K. H. J. Buschow, New class of materials: Half-metallic ferromagnets, Phys. Rev. Lett. **50**, (1983) 2024.

I. Galanakis, P. H. Dederichs, and N. Papanikolaou, Slater-Pauling behavior and origin of the half-metallicity if the full-Heusler alloys, Phys. Rev. B **66**, (2002) 174429.

- <sup>14</sup> Y. Jin, J. Waybright, P. Kharel, I. Tutic, J. Herran, P. Lukashev, S. Valloppilly, and D. J. Sellmyer, Effect of Fe substitution on the structural, magnetic and electron-transport properties of half-metallic Co<sub>2</sub>TiSi, AIP Advances 7, (2017) 055812.
- <sup>15</sup> T. Block, M. J. Carey, B. A. Gurney, O. Jepsen, Band-structure calculations of the half-metallic ferromagnetism and structural stability of full-and half-Heusler phases, Phys. Rev. B **70**, (2004) 205114.
- <sup>16</sup> M. Jourdan, E. Jorge, C. Herbort, M. Kallmayer, P. Klaer, and H. Elmers, Interface and bulk magnetism of Co<sub>2</sub>Cr<sub>0.6</sub>Fe<sub>0.4</sub>Al and Co<sub>2</sub>Cr<sub>A</sub>l thin films, Appl. Phys. Lett. **95**, (2009) 172504.
- Y. Miura, K. Nagao, and M. Shirai, Atomic disorder effects on half-metallicity of the full-Heusler alloys Co<sub>2</sub>(Cr<sub>1-x</sub>Fe<sub>x</sub>)Al: A first-principles study, Phys. Rev. B **69**, (2004) 144413.
- Y. V. Kudryavtsev, V. N. Uvarov, V. A. Oksenenko, Y. P. Lee, J. B. Kim, Y. H. Hyun, K. W. Kim, J. Y. Rhee, and J. Dubowik, Effect of disorder on various physical properties of Co<sub>2</sub>CrAl Heusler alloy films: Experiment and theory, Phys. Rev. B 77, (2008) 195104.
- P. Kharel, J. Herran, P. Lukashev, Y. Jin, J. Waybright, S. Gilbert, B. Staten, P. Gray, S. Valloppilly, Y. Huh, D. J. Sellmyer; Effect of disorder on the magnetic and electronic structure of a prospective spin-gapless semiconductor MnCrVAl, AIP Advances 7, (2017) 056402.
- <sup>20</sup> J. Herran, R. Dalal, P. Gray, P. Kharel, and P. V. Lukashev, Atomic disorder induced modification of magnetization in MnCrVAl, J. Appl. Phys., **122**, (2017) 153904.
- <sup>21</sup> S. Ouardi, G. H. Fecher, C. Felser, and J. Kübler, Realization of Spin Gapless Semiconductors: The Heusler Compound Mn<sub>2</sub>CoAl, Phys. Rev. Lett. **110**, (2013) 100401.
- <sup>22</sup> H. Wu, Y. Qian, W. Tan, C. Xiao, K. Deng, and R. Lu; The theoretical search for half-metallic material: The non-stoichiometric peroskite oxide Sr<sub>2</sub>FeCoO<sub>6-δ</sub>, Appl. Phys. Lett. **99**, (2011) 123116.
- <sup>23</sup> H. van Leuken and R. A. de Groot, Half-metallic antiferromagnets, Phys. Rev. Lett. **74**, (1995) 1171.
- <sup>24</sup> E. Şaşıoğlu, Nonzero macroscopic magnetization in half-metallic antiferromagnets at finite temperatures, Phys. Rev. B **79**, (2009) 100406(R).
- <sup>25</sup> I. Galanakis, and E. Şaşıoğlu, High Tc half-metallic fully-compensated ferrimagnetic Heusler compounds, Appl. Phys. Lett. **99**, (2011) 052509.
- <sup>26</sup> A. Bouabça, H. Rozale, A. Amar, Wang X.T., A. Sayade, A. Lakdja, Half-metallic completely compensated ferrimagnets in Cr doped BaP, Chinese Journal of Physics, **54**, (2016) 489.
- <sup>27</sup> R. Stinshoff, A. K. Nayak, G. H. Fecher, B. Balke, S. Ouardi, Y. Skourski, T. Nakamura, and C. Felser, Completely compensated ferrimagnetism and sublattice spin crossing in the half-metallic Heusler compound Mn<sub>1.5</sub>FeV<sub>0.5</sub>Al, Phys. Rev. B **95**, (2017) 060410(R).
- J. Han, X. Wu, Y. Feng and G. Gao, Half-metallic fully compensated ferrimagnetism and multifunctional spin transport properties of Mn<sub>3</sub>Al, J. Phys.: Condens. Matter 31, (2019) 305501.
- <sup>29</sup> C. Tanaka, J. Nowak, and J. Moodera, Spin-polarized tunneling in a half-metallic ferromagnet, J. Appl. Phys. **86**, (1999) 6239.
- E. O'Leary, A. Ramker, D. VanBrogen, B. Dahal, E. Montgomery, S. Poddar, P. Kharel, A. Stollenwerk, and P. Lukashev, Chemical substitution induced half-metallicity in CrMnSb<sub>1-x</sub>P<sub>x</sub>, J. Appl. Phys., **128**, (2020) 113906.
- <sup>31</sup> P. Blöchl, Projector augmented-wave method, Phys. Rev. B **50**, (1994) 17953.

<sup>32</sup> J. P. Perdew, K. Burke, and M. Ernzerhof, Generalized gradient approximation made simple, Phys. Rev. Lett. **77**, (1996) 3865.

<sup>33</sup> G. Kresse and D. Joubert, From ultrasoft pseudopotentials to the projector augmented-wave method, Phys. Rev. B **59**, (1999) 1758.

<sup>34</sup> M. Methfessel and A. T. Paxton, High-precision sampling for Brillouin-zone integration in metals, Phys. Rev. B **40**, (1989) 3616.

<sup>35</sup> MedeA-2.22, Materials Design, Inc., San Diego, CA, USA, 2017.

<sup>36</sup> M. Meinert, C. Friedrich, G. Reiss, and S. Blügel; *GW* study of the half-metallic Heusler compounds Co<sub>2</sub>MnSi and Co<sub>2</sub>FeSi, Phys. Rev. B **86**, (2012) 245115.

J. Towns, T. Cockerill, M. Dahan, I. Foster, K. Gaither, A. Grimshaw, V. Hazlewood, S. Lathrop, D. Lifka, G. D. Peterson, R. Roskies, J. R. Scott, N. Wilkins-Diehr, "XSEDE: Accelerating Scientific Discovery", Computing in Science & Engineering, vol. 16, no. 5, pp. 62-74, Sept.-Oct. 2014.

<sup>38</sup> B. Dahal, C. Huber, W. Zhang, S. Valloppilly, Y. Huh, P. Kharel, and D. Sellmyer, Effect of partial substitution of In with Mn on the structural, magnetic, and magnetocaloric properties of Ni<sub>2</sub>Mn<sub>1+x</sub>In<sub>1-x</sub> Heusler alloys, J. Phys. D: Appl. Phys. **52**, (2019) 425305.

M. Shaughnessy, L. Damewood, C. Y. Fong, L. H. Yang, and C. Felser, Structural variants and the modified Slater-Pauling curve for transition-metal-based half-Heusler alloys, J. of App. Phys. 113, (2013) 043709.

<sup>40</sup> M.A. Kouacou, A.A. Koua, Z. Yeo, A. Akichi, A. Tanoh and M. Koffi, Magnetic Properties and Electrical Resistivity of Half-Metallic Ferromagnetic Compounds as the Half Heusler PtMnSb, J. Applied Sci., 8 (2008) 682.

<sup>41</sup> J. P. Velev, P. A. Dowben, E. Y. Tsymbal, S. J. Jenkins, and A. N. Caruso, Interface effects in spin-polarized metal/insulator layered structures, Surf. Sci. Rep. **63**, (2008) 400.

<sup>42</sup> K. Waranabe, On New Ferromagnetic Intermetallic Compounds PtMnSn and PtMnSb, J. Phys. Soc. Jpn, **28**, (1970) 302.